



Scientia Research Library

ISSN 2348-0408
USA CODEN: JACOGN

Journal of Applied Chemistry, 2014, 2 (2):1-10

(<http://www.scientiaresearchlibrary.com/archive.php>)

Thermal Expansion and Electrical Conductivity of the $\text{Nd}_{1-x}\text{Sm}_x\text{Ba}_{2-y}\text{Sr}_y\text{Cu}_3\text{O}_{7-\delta}$ Cuprates Solid Solutions at Elevated Temperatures

Andrey I. Klyndyuk^[1], Alexander A. Savitsky^[2]

^[1]Belarusian State Technological University, Sverdlova str., 13A, 220006, Minsk, Belarus,

^[2]Belarusian State University, Nezavisimosti avenue, 4, 220030, Minsk, Belarus

ABSTRACT

It has been found that $\text{Nd}_{1-x}\text{Sm}_x\text{Ba}_{2-y}\text{Sr}_y\text{Cu}_3\text{O}_{7-\delta}$ solid solutions at substitution up to 62,5 mol. % of barium by strontium at any substitution degree of neodymium by samarium are formed. The crystal structure parameters of $\text{Nd}_{1-x}\text{Sm}_x\text{Ba}_{2-y}\text{Sr}_y\text{Cu}_3\text{O}_{7-\delta}$ cuprates have been determined and their oxygen nonstoichiometry, thermal expansion and electrical conductivity within 300–1100 K have been investigated. On the dilatometric curves of cuprates ($\alpha = f(T)$, $\Delta l/l_0 = f(T)$) near 450–550, 800 and 1000 K the anomalies have been observed, which are connected with change of ordering degree and concentration of oxygen vacancies in the $\text{CuO}_{1-\delta}$ -layers of the crystal structure of $\text{Nd}_{1-x}\text{Sm}_x\text{Ba}_{2-y}\text{Sr}_y\text{Cu}_3\text{O}_{7-\delta}$ phases. It has been found that electrical conductivity activation energy of $\text{Nd}_{1-x}\text{Sm}_x\text{Ba}_{2-y}\text{Sr}_y\text{Cu}_3\text{O}_{7-\delta}$ at δ increasing in tetra-phase ($\delta > 0,5$) increased stronger than in ortho-phase ($\delta < 0,5$).

Keywords: Layered perovskites, high-temperature superconductors, solid solutions, crystal structure, existence region, thermal expansion, electrical conductivity.

INTRODUCTION

Layered $\text{LnBa}_2\text{Cu}_3\text{O}_{7-\delta}$ ($\text{Ln} = \text{Y, REE}$) cuprates which are high-temperature superconductors in recent time used in microelectronics (bolometers), medicine (computed tomography) and to create effective systems of accumulation and transfer of energy (superconducting cables, transformers etc.) [1, 2]. The mobility of oxygen subsystem and high electrical conductivity of these oxides at high temperatures allow us to consider them as promising materials for high-temperature electrochemical devices (in particular, solid oxide fuel cells), oxygen membranes, chemical gas sensors, oxidation catalysts as well as thermoelectric generators [3–7].

It is known that properties of $\text{LnBa}_2\text{Cu}_3\text{O}_{7-\delta}$ depend on their oxygen content ($7-\delta$) and on the ordering degree of oxygen vacancies in the $-\text{CuO}_{1-\delta}$ - layers of their crystal structure [8–10]. “ $T - \delta$ ” phase diagrams of $\text{LnBa}_2\text{Cu}_3\text{O}_{7-\delta}$ cuprates are studied in detail [2, 8] but literature data about phase transitions in $\text{LnBa}_2\text{Cu}_3\text{O}_{7-\delta}$ oxides are scarce and sometimes contradictory. So, according dilatometry results, $\text{YBa}_2\text{Cu}_3\text{O}_{7-\delta}$ cuprate undergoes structural transitions near 500 [11], 673 [12],

470 K [9, 13] и 700 [11], 973 [12], 780 K [9,13]. High-temperature anomaly corresponds to the $O2 \rightarrow T$ transition (orthorhombic 2 \rightarrow tetragonal phase), but low-temperature one takes place due to the $O1 \rightarrow O2$ transition (orthorhombic 1 \rightarrow orthorhombic 2 phases) which is connected with reordering of oxygen vacancies in $-CuO_{1-\delta}-$ layeres. In the works [14–18] on the basis of results of investigation of thermo- and electrophysical properties of $LnBa_2Cu_3O_{7-\delta}$ phases it was found that temperature and intensity of anomalies of cuprates properties depended on their cationic composition and thermal prehistory.

Of great interest are the cuprates of light REE ($Ln = Nd, Sm$) and barium in which fixed so-called peak-effect or maximum on the curves $J_c = f(H)$ in the region of magnetic fields of 1–5 T [19, 20] (abnormal increase of the critical current density in the region of small magnetic fields). The presence of the peak-effect in these phases one can associate with various defects in their crystal structure having different nature (dislocations, twin boundaries etc. as well as nanoscale regions with different nonstoichiometry of cations and oxygen which formed in result, for example, spinodal decomposition of superconducting cuprates) [2, 21].

In this work continuing our studies of superconducting $LnBa_2Cu_3O_{7-\delta}$ cuprates [9, 13–18] the results of investigation of $Nd_{1-x}Sm_xBa_{2-y}Sr_yCu_3O_{7-\delta}$ are presented; existence region of $Nd_{1-x}Sm_xBa_{2-y}Sr_yCu_3O_{7-\delta}$ solid solutions is established, parameters of their crystal structure are determined and within wide temperature range thermal stability, thermal expansion and electrical conductivity of $Nd_{1-x}Sm_xBa_{2-y}Sr_yCu_3O_{7-\delta}$ oxides are studied.

MATERIALS AND METHODS

The powders of $Nd_{1-x}Sm_xBa_{2-y}Sr_yCu_3O_{7-\delta}$ phases ($x = 0,00–1,00$, $y = 0,00–1,75$ with increment of 0,25) using ceramic method from Nd_2O_3 (chemically pure grade), Sm_2O_3 (chemically pure grade), CuO (ultra pure grade), $BaCO_3$ (pure grade) and $SrCO_3$ (pure grade) in air within 1173–1223 K were prepared [9, 13]. For measurements of thermal expansion and electrical conductivity of the samples from the powders obtained the pellets having diameter of 9 mm and thickness of 3–5 mm and bars having dimensions 5x5x30 mm were pressed and then sintered in air at 1223 K during 10 h. The density of ceramics after sintering was 80 to 90% of the theoretical value. Before studies the powder and ceramic samples for saturation of them by oxygen were annealed in flow of oxygen for 5 to 10 hours at 723 K followed by cooling (cooling rate of $2–5\text{ K}\cdot\text{min}^{-1}$) to room temperature in the flow of oxygen ($P_{O_2} = 1,01\cdot 10^5\text{ Pa}$).

X-ray diffraction analysis (XRD) of the samples on the DRON–3 diffractometer ($CuK\alpha$ -radiation, Ni-filter) at room temperature was performed. Oxygen content in the samples was determined iodometrically [9]. Thermal stability of $Nd_{1-x}Sm_xBaSrCu_3O_{7-\delta}$ phases at low partial pressure of oxygen ($P_{O_2} = 15\text{ Pa}$) by means of measuring complex OXYLYT (SensoTech, Germany) was investigated [22]. Thermal expansion of the $Nd_{1-x}Sm_xBaSrCu_3O_{7-\delta}$ oxides was studied using dilatometry [13, 14] in air ($P_{O_2} = 2,10\cdot 10^4\text{ Pa}$) within 300–1100 K in a dynamic mode with heating–cooling rate of $3–5\text{ K}\cdot\text{min}^{-1}$. Electrical conductivity of the sintered ceramics by means of four-probe method (direct current) in oxygen ($P_{O_2} = 1,01\cdot 10^5\text{ Pa}$), air ($P_{O_2} = 2,10\cdot 10^4\text{ Pa}$) and in argon ($P_{O_2} = 15\text{ Pa}$) within 300–1100 K was measured [15, 16]. Partial pressure of oxygen (P_{O_2}) in the measuring system during measurements using “Zircon–M” was monitored. Before measurements of electrical properties of the samples on their surface the Ag-electrodes were formed by means of burning of silver paste at 1073 K during 5 min.

RESULTS AND DISCUSSIONS

According to the XRD results the monophase $\text{Nd}_{1-x}\text{Sm}_x\text{Ba}_{2-y}\text{Sr}_y\text{Cu}_3\text{O}_{7-\delta}$ solid solutions are formed at $y \leq 1,25$ at any x . On the XRD patterns of the samples having strontium content more than 62,5 mol. % the reflexes of additional $\text{Ln}_2\text{BaCuO}_5$ ($\text{Ln} = \text{Nd}, \text{Sm}$), BaCuO_2 and CuO phases were observed. After final stage of annealing in oxygen ($P_{\text{O}_2} = 1,01 \cdot 10^5 \text{ Pa}$) all the solid solutions had orthorhombic structure with lattice constants of $a = 0,3780 \pm 0,3879 \text{ nm}$, $b = 0,3835 \pm 0,3922 \text{ nm}$, $c = 1,151 \pm 1,177 \text{ nm}$, $V = (167,2 \pm 179,1) \cdot 10^{-3} \text{ nm}^3$ (see table 1).

Determined by us width of the homogeneity region of the $\text{Nd}_{1-x}\text{Sm}_x\text{Ba}_{2-y}\text{Sr}_y\text{Cu}_3\text{O}_{7-\delta}$ solid solutions ($0,00 \leq x \leq 1,00$; $0,00 \leq y \leq 1,25$) is in good agreement with the literature data according to them the monophase samples of the $\text{LnBa}_{2-y}\text{Sr}_y\text{Cu}_3\text{O}_{7-\delta}$ solid solutions at substitution of barium by strontium up to 50–65 mol. % are formed [8, 9, 14].

As can be seen from the data given in the table 1 and on the fig. 1, substitution of barium by strontium in layered neodymium–samarium and barium cuprates leads to the linear decreasing of the lattice constants of the $\text{Nd}_{1-x}\text{Sm}_x\text{Ba}_{2-y}\text{Sr}_y\text{Cu}_3\text{O}_{7-\delta}$ solid solutions and increasing of the values of tetragonal

($\varepsilon = \frac{2 \cdot c}{3 \cdot (a + b)}$) and orthorhombic distortion degree ($\eta = \frac{2 \cdot (b - a)}{b + a}$) of their crystal structure.

Lattice constants of the $\text{Nd}_{1-x}\text{Sm}_x\text{Ba}_{2-y}\text{Sr}_y\text{Cu}_3\text{O}_{7-\delta}$ solid solutions at substitution of neodymium by samarium change slightly due to the closing of ionic radii of Nd^{3+} and Sm^{3+} (according to the [23], for C.N. = 6 ionic radii of Nd^{3+} , Sm^{3+} , Ba^{2+} and Sr^{2+} ions are 0,104, 0,100, 0,134 and 0,112 nm respectively).

Table 1:-Values of oxygen nonstoichiometry index (δ) and lattice constants (a , b , c , V) of the $\text{Nd}_{1-x}\text{Sm}_x\text{Ba}_{2-y}\text{Sr}_y\text{Cu}_3\text{O}_{7-\delta}$ cuprates solid solutions

| x | y | δ | a , nm | b , nm | c , nm | V , nm ³ |
|------|------|----------|----------|----------|----------|-----------------------|
| 0,00 | 0,00 | 0,06 | 0,3879 | 0,3922 | 1,177 | 0,1791 |
| | 0,50 | 0,11 | 0,3873 | 0,3881 | 1,164 | 0,1750 |
| | 0,75 | 0,14 | 0,3821 | 0,3867 | 1,160 | 0,1714 |
| | 1,00 | 0,18 | 0,3809 | 0,3863 | 1,159 | 0,1705 |
| | 1,25 | 0,21 | 0,3798 | 0,3859 | 1,158 | 0,1697 |
| 0,25 | 0,00 | 0,07 | 0,3851 | 0,3902 | 1,171 | 0,1760 |
| | 0,25 | 0,09 | 0,3843 | 0,3900 | 1,170 | 0,1753 |
| | 0,50 | 0,11 | 0,3832 | 0,3892 | 1,167 | 0,1740 |
| | 0,75 | 0,15 | 0,3813 | 0,3876 | 1,163 | 0,1719 |
| | 1,00 | 0,19 | 0,3802 | 0,3867 | 1,160 | 0,1705 |
| | 1,25 | 0,21 | 0,3791 | 0,3851 | 1,155 | 0,1686 |
| 0,50 | 0,00 | 0,06 | 0,3857 | 0,3904 | 1,171 | 0,1763 |
| | 0,25 | 0,09 | 0,3842 | 0,3890 | 1,167 | 0,1744 |
| | 0,50 | 0,11 | 0,3830 | 0,3877 | 1,163 | 0,1727 |
| | 0,75 | 0,14 | 0,3816 | 0,3869 | 1,161 | 0,1714 |
| | 1,00 | 0,18 | 0,3803 | 0,3859 | 1,158 | 0,1699 |
| | 1,25 | 0,20 | 0,3791 | 0,3850 | 1,155 | 0,1686 |
| 0,75 | 0,00 | 0,07 | 0,3847 | 0,3898 | 1,169 | 0,1753 |

| | | | | | | |
|------|------|------|--------|--------|-------|--------|
| | 0,25 | 0,09 | 0,3827 | 0,3890 | 1,167 | 0,1737 |
| | 0,50 | 0,12 | 0,3821 | 0,3874 | 1,162 | 0,1720 |
| | 0,75 | 0,15 | 0,3812 | 0,3860 | 1,158 | 0,1704 |
| | 1,00 | 0,19 | 0,3804 | 0,3851 | 1,155 | 0,1692 |
| | 1,25 | 0,21 | 0,3791 | 0,3842 | 1,153 | 0,1679 |
| 1,00 | 0,00 | 0,07 | 0,3842 | 0,3890 | 1,167 | 0,1744 |
| | 0,25 | 0,10 | 0,3823 | 0,3881 | 1,164 | 0,1727 |
| | 0,50 | 0,12 | 0,3815 | 0,3867 | 1,160 | 0,1711 |
| | 0,75 | 0,15 | 0,3807 | 0,3853 | 1,156 | 0,1696 |
| | 1,00 | 0,19 | 0,3800 | 0,3845 | 1,153 | 0,1685 |
| | 1,25 | 0,22 | 0,3788 | 0,3835 | 1,151 | 0,1672 |

It should be note that perovskite unit cell parameter a_p ($a_p = \sqrt[3]{V/3}$) of $\text{Nd}_{1-x}\text{Sm}_x\text{Ba}_{2-y}\text{Sr}_y\text{Cu}_3\text{O}_{7-\delta}$ cuprates solid solutions linearly depends practically on the value of mean radius of cations

\bar{R} ($\bar{R} = \sum_{i=1}^n x_i \cdot R_i$), where x_i and R_i – part of A–position filled by i –th cation and its ionic radius

[23]), situated in A–positions (Nd/Sm, Ba/Sr) of these phases crystal structure (fig. 2). So we can conclude that sizes of cations situated in positions of Ln^{3+} and Ba^{2+} in the crystal structure of $\text{LnBa}_2\text{Cu}_3\text{O}_{7-\delta}$ phases average almost equally effect the size of the unit cell of these phases.

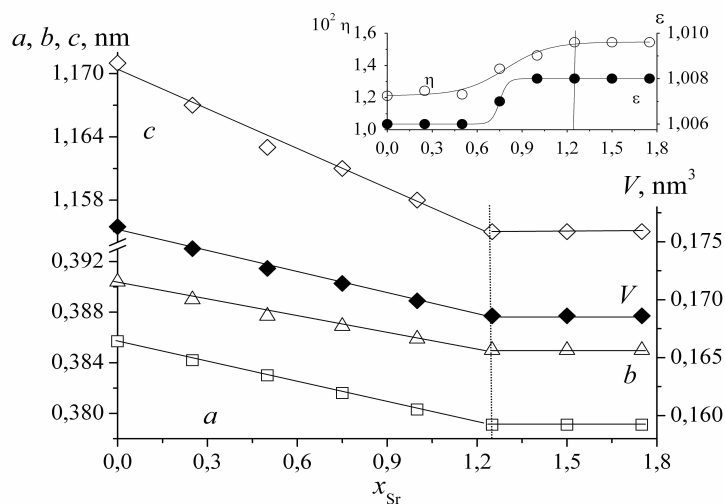


Fig. 1. Dependences of lattice constants (a , b , c , V) and tetragonal (ϵ) and orthorhombic distortion degree (η) of the unit cell of the $\text{Nd}_{0.5}\text{Sm}_{0.5}\text{Ba}_{2-y}\text{Sr}_y\text{Cu}_3\text{O}_{7-\delta}$ solid solutions on substitution degree of barium by strontium. Vertical dotted line shows the solubility limit of Sr in $\text{Nd}_{0.5}\text{Sm}_{0.5}\text{Ba}_{2-y}\text{Sr}_y\text{Cu}_3\text{O}_{7-\delta}$

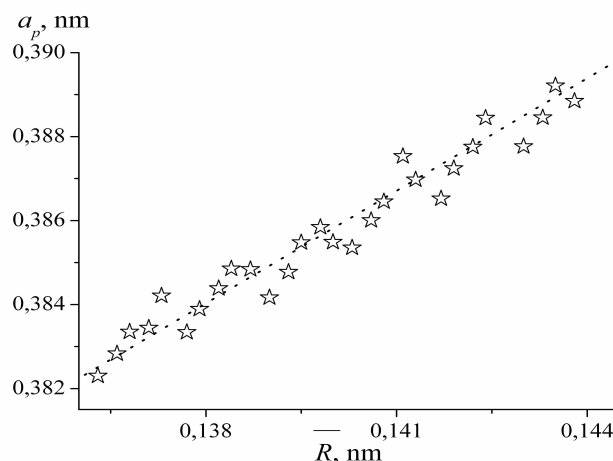


Fig. 2. Dependence of perovskite unit cell parameter (a_p) on mean ionic radius value (\bar{R}) of cations situated in A-positions of crystal structure of $\text{Nd}_{1-x}\text{Sm}_x\text{Ba}_{2-y}\text{Sr}_y\text{Cu}_3\text{O}_{7-\delta}$ cuprates

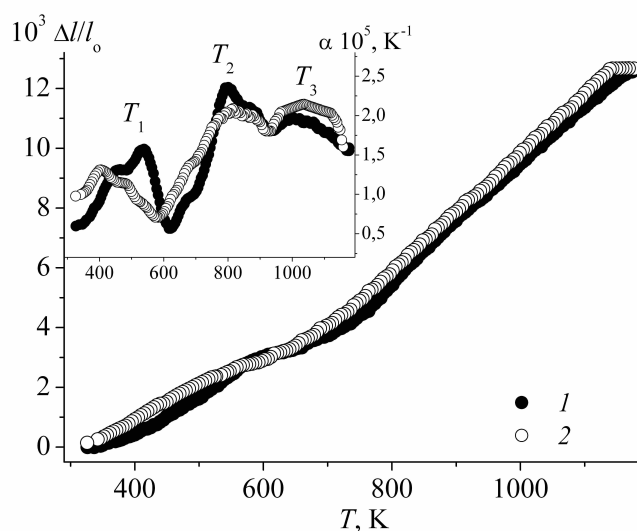


Fig. 3. Temperature dependences of the relative elongation ($\Delta l/l_0$) and true linear thermal expansion coefficient (α) of the $\text{Nd}_{0.25}\text{Sm}_{0.75}\text{Ba}_2\text{Cu}_3\text{O}_{7-\delta}$ solid solution: 1 – heating, 2 – cooling

Values of oxygen nonstoichiometry index (δ) of $\text{Nd}_{1-x}\text{Sm}_x\text{Ba}_{2-y}\text{Sr}_y\text{Cu}_3\text{O}_{7-\delta}$ phases determined by means of iodometry varied from 0.06–0.07 for the samples without strontium up to 0.20–0.22 for the samples with substitution of barium by strontium on 62.5 mol. % (table 1) which are also in a good accordance with the literature data [8, 9].

On the dilatometric curves (fig. 3) of $\text{Nd}_{1-x}\text{Sm}_x\text{Ba}_{2-y}\text{Sr}_y\text{Cu}_3\text{O}_{7-\delta}$ cuprates during thermocycling (heating and cooling) the small hysteresis was observed which took place due to the difficulty of oxygen exchange between the samples and environment [8, 9, 13]. On the temperature dependences of the relative elongation ($\Delta l/l_0 = f(T)$) and linear thermal expansion coefficient (LTEC) ($\alpha = f(T)$) (fig. 3) of the $\text{Nd}_{1-x}\text{Sm}_x\text{Ba}_{2-y}\text{Sr}_y\text{Cu}_3\text{O}_{7-\delta}$ phases three pronounced anomalies were observed: wide anomaly within temperature region of 450–550 K (T_1) and narrower near 800 (T_2) and 1000 K (T_3). These anomalies correspond to the phase transition O1 ($\delta < 0.25$) → O2 ($\delta \approx 0.25$) (T_1), O2 ($\delta \approx 0.25$) → T ($\delta \approx 0.50$)

(T_2) and T ($\delta \approx 0,50$) \rightarrow high-temperature phase (H, $\delta \approx 0,75$) (T_3) due to the disordering of oxygen vacancies and increasing of their concentration in the $-\text{CuO}_x-$ layers of crystal structure of $\text{Nd}_{1-x}\text{Sm}_x\text{Ba}_{2-y}\text{Sr}_y\text{Cu}_3\text{O}_{7-\delta}$ cuprates [9, 14, 17].

As can be seen from the data given in the table 2 LTEC value of the $\text{Nd}_{1-x}\text{Sm}_x\text{Ba}_{2-y}\text{Sr}_y\text{Cu}_3\text{O}_{7-\delta}$ phases decreases at substitution of barium by strontium and slightly increases at substitution of neodymium by samarium. These results show that substitution $\text{Sr}^{2+} \rightarrow \text{Ba}^{2+}$ leads to the increasing but intersubstitution REE ($\text{Sm}^{3+} \leftrightarrow \text{Nd}^{3+}$) on the contrary to the decreasing of the strength of the crystal structure of $\text{Nd}_{1-x}\text{Sm}_x\text{Ba}_{2-y}\text{Sr}_y\text{Cu}_3\text{O}_{7-\delta}$ phases which is in a good accordance with the results of works [13, 18].

On the fig. 4 the $\alpha - T - x$ diagram of the $\text{Nd}_{1-x}\text{Sm}_x\text{Ba}_2\text{Cu}_3\text{O}_{7-\delta}$ solid solutions is given (the $\alpha - T - x(y)$ diagrams of other series of solid solutions in the $\text{Nd}_{1-x}\text{Sm}_x\text{Ba}_{2-y}\text{Sr}_y\text{Cu}_3\text{O}_{7-\delta}$ system look like it). As can be seen from the fig. 4, on the concentration dependences of LTEC at phase transitions $\text{O1} \rightarrow \text{O2}$, $\text{O2} \rightarrow \text{T}$ and $\text{T} \rightarrow \text{H}$ the pronounced anomalies (extrema) are observed. These anomalies correspond to the substitution degree of neodymium by samarium on 50 mol. % and barium by strontium on 25 and 50 mol. %. The such anomalies were observed by us earlier at the study of thermal expansion of $\text{YBa}_{2-x}\text{Me}_x\text{Cu}_3\text{O}_{7-\delta}$ ($\text{Me} = \text{Sr}, \text{Ca}$) solid solutions [9, 13]. Taking into account

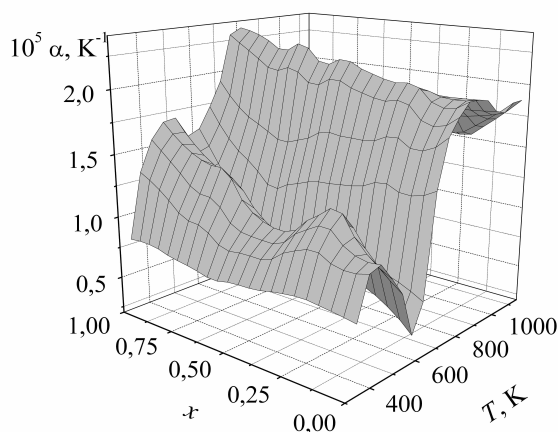


Fig. 4. $\alpha - T - x$ diagram of the $\text{Nd}_{1-x}\text{Sm}_x\text{Ba}_2\text{Cu}_3\text{O}_{7-\delta}$ solid solutions

the results of [13] the anomalies which were found in this work on dependences $\alpha = f(x)$ ($\alpha = f(y)$) for $\text{Nd}_{1-x}\text{Sm}_x\text{Ba}_{2-y}\text{Sr}_y\text{Cu}_3\text{O}_{7-\delta}$ solid solution can be explained by partial ordering of Nd^{3+} and Sm^{3+} , Ba^{2+} and Sr^{2+} cations in the positions of Ln^{3+} and Ba^{2+} of crystal structure of these phases.

Table 2 :-Values of the true linear thermal expansion coefficient (LTEC, α) of the $\text{Nd}_{1-x}\text{Sm}_x\text{Ba}_{2-y}\text{Sr}_y\text{Cu}_3\text{O}_{7-\delta}$ cuprates solid solutions at different temperatures

| x | y | $\alpha \cdot 10^5, \text{K}^{-1}$ | | | |
|------|------|------------------------------------|-------|-------|--------|
| | | 400 K | 600 K | 800 K | 1000 K |
| 0,00 | 0,00 | 1,55 | 1,49 | 2,40 | 1,57 |
| | 0,50 | 0,97 | 1,05 | 2,07 | 1,72 |
| | 1,00 | 1,12 | 0,04 | 1,97 | 1,71 |
| | 1,25 | 1,06 | 0,73 | 2,19 | 1,57 |
| 0,25 | 0,00 | 0,92 | 1,62 | 2,73 | 1,64 |
| | 0,25 | 1,43 | 1,24 | 2,19 | 1,60 |
| | 0,50 | 1,38 | 1,38 | 1,87 | 1,83 |

| | | | | | |
|------|------|------|------|------|------|
| | 0,75 | 1,07 | 1,15 | 2,21 | 1,88 |
| | 1,00 | 0,93 | 0,43 | 2,07 | 1,99 |
| | 1,25 | 0,90 | 0,58 | 1,87 | 1,71 |
| 0,50 | 0,00 | 1,44 | 1,48 | 2,81 | 1,74 |
| | 0,25 | 1,40 | 1,36 | 1,69 | 1,90 |
| | 0,50 | 1,50 | 1,48 | 2,76 | 1,91 |
| | 0,75 | 0,73 | 0,91 | 2,46 | 1,90 |
| | 1,00 | 0,53 | 0,43 | 2,23 | 1,91 |
| | 1,25 | 1,23 | 1,21 | 1,71 | 1,28 |
| 0,75 | 0,00 | 1,18 | 1,41 | 2,86 | 1,64 |
| | 0,25 | 0,93 | 1,33 | 1,84 | 1,94 |
| | 0,50 | — | 1,86 | 1,30 | 2,12 |
| | 0,75 | 0,51 | 0,81 | 2,48 | 1,96 |
| | 1,00 | 0,89 | 0,67 | 2,37 | 2,12 |
| | 1,25 | 1,01 | 0,62 | 2,06 | 1,93 |
| 1,00 | 0,00 | 0,86 | 0,51 | 2,10 | 1,84 |
| | 0,25 | 1,11 | 0,79 | 1,70 | 1,90 |
| | 0,50 | 0,95 | 1,04 | 1,47 | 1,70 |
| | 1,00 | 1,23 | 1,44 | 2,60 | 1,72 |
| | 1,25 | 0,57 | 1,36 | 1,61 | 1,98 |

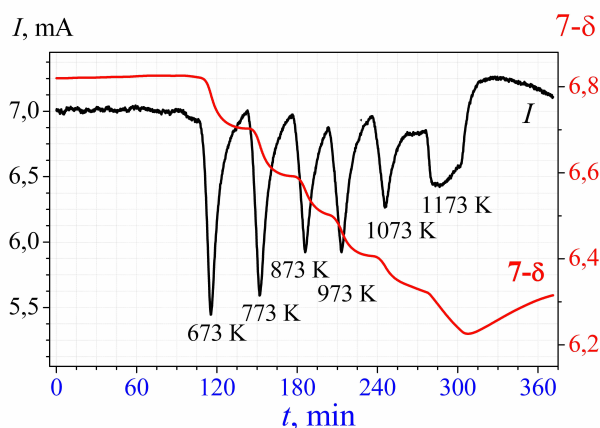


Fig. 5. Change of oxygen nonstoichiometry ($7-\delta$) of the $\text{Nd}_{0.5}\text{Sm}_{0.5}\text{BaSrCu}_3\text{O}_{7-\delta}$ during heating and cooling in argon ($P_{\text{O}_2} = 15 \text{ Pa}$) (I – titration)

On the fig.5 the results of investigation of thermal stability and oxygen nonstoichiometry of $\text{Nd}_{0.5}\text{Sm}_{0.5}\text{BaSrCu}_3\text{O}_{7-\delta}$ cuprate are presented. As it is seen at low oxygen content in atmosphere the intensity of oxygen evolution from the sample monotonously decreases at temperature increasing (δ increasing) but oxygen content in the samples ($7-\delta$) linearly decreases practically at temperature increasing.

Electrical conductivity (σ) of the $\text{Nd}_{1-x}\text{Sm}_x\text{Ba}_{2-y}\text{Sr}_y\text{Cu}_3\text{O}_{7-\delta}$ solid solutions in oxygen and in air within all the temperature interval studied had metallic character ($\partial\sigma/\partial T < 0$) and more strongly decreased at $T > 700$ K that was connected with the evolution of oxygen from the samples into environment and decreasing of concentration of main charge carriers – “holes” ($\text{O}^{2-} \rightarrow \frac{1}{2}\text{O}_2 + 2e, e + p \rightarrow 0$) [3,9,15–18].

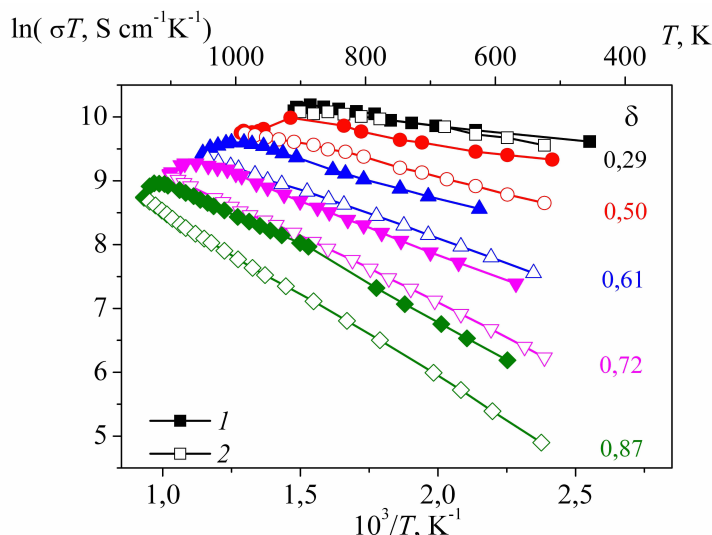


Fig. 6. Temperature dependences of electrical conductivity of $\text{Nd}_{0.25}\text{Sm}_{0.75}\text{Ba}_2\text{Cu}_3\text{O}_{7-\delta}$ solid solution having different oxygen content ($7-\delta$) in argon ($P_{\text{O}_2} = 15$ Pa) during heating (1) and cooling (2)

At increasing of oxygen content in the samples their conductivity character changed from metallic to semiconducting ($\partial\sigma/\partial T > 0$). The values of apparent activation energy of electrical conductivity (E_A) of cuprates calculated from $\ln(\sigma \cdot T) = f(1/T)$ dependences (fig. 6) monotonously increased at increasing of values of their oxygen nonstoichiometry (δ) (fig. 7) that was in a good agreement with the results obtained by us earlier during study of electrical conductivity of $\text{Y}_{1-x}\text{M}_x\text{Ba}_2\text{Cu}_3\text{O}_{7-\delta}$ ($M = \text{Bi}, \text{Ca}$) [15, 16] and $\text{Nd}_{1-x}\text{Tm}_x\text{Ba}_2\text{Cu}_3\text{O}_{7-\delta}$ solid solutions [18]. On the $E_A = f(T)$ dependence (fig. 7) for the cuprates studied two sharply pronounced parts are observed: in ortho-phase (O, $\delta < 0.5$) at δ increasing E_A increases less intensively than in tetra-phase (T, $\delta > 0.5$). So we can conclude that processes of charge transfer in T-phase of $\text{LnBa}_2\text{Cu}_3\text{O}_{7-\delta}$ type cuprates go with more energetical difficulties than in O-phase.

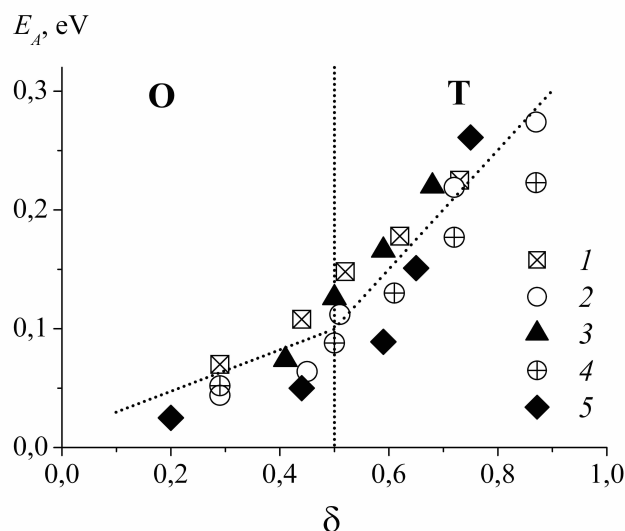


Fig. 7. Dependence of activation energy of electrical conductivity of $\text{Nd}_{1-x}\text{Sm}_x\text{Ba}_2\text{Cu}_3\text{O}_{7-\delta}$ solid solutions in argon ($P_{\text{O}_2} = 15 \text{ Pa}$) versus their oxygen nonstoichiometry index (δ): $x = 0,00$ (1), $0,25$ (2), $0,50$ (3), $0,75$ (4), $1,00$ (5). O and T – regions existence of orthorhombic ($\delta < 0,5$) and tetragonal ($\delta > 0,5$) modifications of $\text{Nd}_{1-x}\text{Sm}_x\text{Ba}_{2-y}\text{Sr}_y\text{Cu}_3\text{O}_{7-\delta}$ cuprates

CONCLUSION

So in this work the existence region of $\text{Nd}_{1-x}\text{Sm}_x\text{Ba}_{2-y}\text{Sr}_y\text{Cu}_3\text{O}_{7-\delta}$, was established, their lattice constants were determined and within temperature region 300–1100 K their oxygen nonstoichiometry, thermal expansion and electrical conductivity were investigated. The anomalies of thermal expansion of the samples connected with the ordering of ions in anionic (oxygen) and A-cationic sublattices of their crystal structure were detected. It was found that charge transfer in O-phase of $\text{Nd}_{1-x}\text{Sm}_x\text{Ba}_{2-y}\text{Sr}_y\text{Cu}_3\text{O}_{7-\delta}$ cuprates was energetically less difficult than in T-phase.

ACKNOWLEDGEMENT

Authors are grateful to the V.V. Vashook and O.I. Kirilenko (IGIC NASB) for organization and carrying of investigation of $\text{Nd}_{1-x}\text{Sm}_x\text{Ba}_{2-y}\text{Sr}_y\text{Cu}_3\text{O}_{7-\delta}$ powders on the measuring complex OXYLYT. This work was carried out at partial financial support of Belarusian Republican Foundation for Fundamental Research (grant X97M–005).

REFERENCES

- [1]. Iguchi I., Lee K., *Mat. Sci. & Eng. B*, **1996**, 41, 1, 76–82.
- [2]. Tretyakov Yu.D., Goodilin E.A., *Russian Chemical Reviews*, **2000**, 69, 1, 1–40.
- [3]. Nowotny J., Pekas M., Weppner W., *J. Amer. Ceram. Soc.*, **1990**, 73, 4, 1040–1047.
- [4]. Hu J., Hu X., Hao H., Guo L., Song H., Yang D., *Solid State Ionics*, **2005**, 176, 487–494.
- [5]. Abou–Sekkina M. M., *Mat. Lett.*, **2000**, 42, 297–304.
- [6]. Akhalbedashvili L.G., Alapishvili M.G., Davituliani I.P., Kekelidze N.P., Petviashvili D.G., Sarishvili Ts.G., *Rus. J. Phys. Chem.*, **2001**, 75, 10, 1619–1621.

-
- [7]. Rodriguez J.E., Lopez J., *Physica B*, **2007**, 387, 143–146.
- [8]. Fotijev A.A., Slobodin B.V., Fotijev V.A., *High-Temperature Superconductors Chemistry and Technology*. Ekaterinburg, **1993** p.
- [9]. Klyndyuk A.I., PhD thesis, Belarus State Technological University (Minsk, Belarus, **2001**).
- [10]. Ng H.K., Mathias H., Moulton W.G., Pan K.K., Pan S.J., Rey C.M., Testardi L.R., *Solid State Commun.*, **1988**, 65, 1, 63–66.
- [11]. Basargin O.V., Rudnitsky L.A., Moshchalkov V.V., Kaul A.R., Graboy I.E., Tretyakov Yu.D., *Physics of the Solid State*, **1988**, 30, 877–879.
- [12]. Szytula A., Mavrodiev G., Koneska S., Fukarowa–Jurukowska M., *Acta Phys. Pol.*, **1988**, A73, 785–788.
- [13]. Petrov G.S., Klyndyuk A.I., Massyuck S.V., Bashkirov L.A., Akimov A.I., *High Temp. – High Press.*, **1998**, 30, 483–488.
- [14]. Klyndyuk A.I., Petrov G.S., Bashkirov L.A., *J. Mat. Sci.*, **2002**, 37, 5381–5386.
- [15]. Savitsky A.A., Klyndyuk A.I., *Vestnik BSU, Ser. 2*, **2004**, 3, 7–13.
- [16]. Savitsky A.A., Klyndyuk A.I., *Vestnik BSU, Ser. 2*, **2006**, 2, 20–24.
- [17]. Klyndyuk A.I., Petrov G.S., Poluyan A.F., Bashkirov L.A., *Proc. NASB, Chem. Ser.*, **2006**, 1, 5–9.
- [18]. Klyndyuk A.I., Petrov G.S., Akimov A.I., Dalidovich S.V., Savitsky A.A., *Proc. NASB, chem. ser.*, **2006**, 4, 5–9.
- [19]. Murakami M., Yoo S.I., Higuchi T., Sakai N., *J. Appl. Phys.*, **1994**, 33, 715–717.
- [20]. Murakami M., Sakai N., Higuchi T., Yoo S.I., *Supercond. Sci. Technol.*, **1996**, 9, 1015–1032.
- [21]. Suematsu H., Kawano M., Onda T., *Physica C*, **1999**, 324, 161–171.
- [22]. Bode M., Teske K., Ullmann K., *Fachzeitschrift für Laboratorium*, **1994**, 38, 495–500.
- [23]. Shannon R.D., Prewitt C. T., *Acta Cryst.*, **1969**, B25, 5, 946–960.